Silent Positioning in Underwater Acoustic Sensor Networks

Xiuzhen Cheng, *Member, IEEE*, Haining Shu, *Student Member, IEEE*, Qilian Liang, *Senior Member, IEEE*, and David Hung-Chang Du, *Fellow, IEEE*

***Abstract*—In this paper, we present a silent positioning scheme termed UPS for underwater acoustic sensor networks. UPS relies on the time difference of arrivals locally measured at a sensor to detect range differences from the sensor to four anchor nodes. These range differences are averaged over multiple beacon intervals before they are combined to estimate the 3-D sensor location through trilateration. UPS requires no time synchronization and provides location privacy at underwater vehicles/sensors whose locations need to be determined. To study the performance of UPS, we model the underwater acoustic channel as a modified ultrawideband Saleh–Valenzuela model: The arrival of each path cluster and the paths within each cluster follow double Poisson distributions, and the multipath channel gain follows a Rician distribution. Based on this channel model, we perform both theoretical analysis and simulation study on the position error of UPS under acoustic fading channels. The obtained results indicate that UPS is an effective scheme for underwater vehicle/sensor self-positioning.**

***Index Terms*—Localization, navigation, UnderWater Acoustic Sensor Networks (UWA-SNs), underwater Global Positioning System (GPS), underwater positioning, ultrawideband (UWB) Saleh–Valenzuela (S-V) model.**

I. Introduction

UNDERWATER Acoustic Sensor Networks (UWA-SNs) consist of a variable number of sensors and vehicles (the unmanned underwater vehicle (UUV), the autonomous underwater vehicle (AUV), etc.) to perform collaborative monitoring tasks over a given area. The main motivation for UWA-SNs is their relative ease of deployment since they eliminate the need for cables, and they do not interfere with shipping activities. UWA-SNs are envisioned to enable applications for environmental monitoring of physical and chemical/biological indicators, tactical surveillance, disaster prevention, undersea exploration, assisted navigation, etc.

Location discovery for underwater vehicles/sensors is nontrivial in the oceanic medium. Propagation delays, motion-induced Doppler shift, phase and amplitude fluctuations, multipath interference, etc. are all significant factors in location measurement. The well-known Global Positioning System (GPS) receivers, which may be used in terrestrial systems to accurately estimate the geographical locations of sensor nodes, do not work properly underwater [7]. Some localization schemes based on received signal strength (RSS), time of arrival (ToA), or angle of arrival (AoA) could be used. Nevertheless, the bandwidth constraint, sensor mobility, and unpredicted variation in channel behavior make many of these approaches inaccurate or unapplicable [15]. For example, the Doppler shift introduced by mobility affects the AoA algorithm, and the underwater power loss model (depending on distance and frequency) makes the RSS-based estimation results ambiguous. Moreover, the accuracy of the localization relates to the bandwidth of the signal and the signal-to-noise ratio at the receiver [5, p. 429]. The lower limit for σ^2 estimation in the presence of additive white Gaussian noise is given by the Cramer–Rao lower bound, i.e., $\sigma^2 = (N_0/2 \int_{-\infty}^{+\infty} (2\pi f)^2 |p(f)|^2 df)$, which indicates that σ^2 is inversely proportional to the bandwidth. Unfortunately, the bandwidth of UWA-SNs is significantly limited, which theoretically demonstrates that acoustic positioning in UWA-SNs is very challenging.

Intuitively, ToA- or time difference of arrival (TDoA)-based localization should be preferable. Nevertheless, ToA or TDoA approaches require time synchronization if one-way sound flying time is counted on; otherwise, a ping-pong-style round-trip propagation delay needs to be measured. In UWA-SNs, precise time synchronization is hard to achieve due to the characteristics of sound when traveling in water [29]. In addition, the low bandwidth of acoustic signals is shared by navigation and data communication in UWA-SNs [26]; therefore, the ping-pong-style alternative may significantly decrease the network throughput. For the same reason, schemes requiring a large number of anchor nodes whose locations are known *a priori* are prohibitive to UWA-SN. In this paper, we propose UPS, which is a ToA-based silent underwater positioning scheme, to carefully address the concerns and challenges previously mentioned.

The major contribution of this paper lies in three aspects: First, we propose UPS, i.e., a silent positioning scheme for UWA-SNs, and demonstrate our algorithm by simulation.

Manuscript received March 25, 2007; revised July 26, 2007 and September 13, 2007. The work of X. Cheng was supported in part by the National Science Foundation (NSF) under Grants CNS-0347674 and CNS-0721669. The work of H. Shu and Q. Liang was supported in part by the NSF under Grant CNS-0721515 and in part by the Office of Naval Research under Grants N00014-07-1-0395 and N00014-07-1-1024. The review of this paper was coordinated by Prof. X. Shen.

X. Cheng is with the Department of Computer Science, The George Washington University, Washington, DC 20052 USA (e-mail: cheng@gwu.edu).

H. Shu and Q. Liang are with the Department of Electrical Engineering, The University of Texas at Arlington, Arlington, TX 76019 USA (e-mail: shu@wcn.uta.edu; liang@uta.edu).

D. H.-C. Du is with the Department of Computer Science and Engineering, University of Minnesota, Minneapolis, MN 55455 USA (e-mail: du@cs.umn.edu).

Color versions of one or more of the figures in this paper are available online at http://ieeexplore.ieee.org.

Digital Object Identifier 10.1109/TVT.2007.912142

Second, we investigate the propagation delay and multipath channel. We found that, in acoustic underwater networks with large propagation delays, a multipath channel can be modeled as a modified ultrawideband (UWB) Saleh–Valenzuela (S-V) model: The arrival of each cluster and the paths within each cluster follow double Poisson distributions, and the multipath channel gain follows a Rician distribution. Third, we analyze the theoretical performance of our scheme in propulsion noise environments and identify the possible sources of errors with measures to help mitigate them. Compared to existing schemes proposed in the context of UWA-SNs, UPS has five characteristics and advantages.

1) UPS utilizes very few anchor nodes (four anchors in our study) and requires no special hardware to provide 3-D localization.
2) UPS requires no time synchronization. All time differences are computed from the measurements by a local timer.
3) UPS provides *silent positioning*. Underwater vehicles and sensors do not actively transmit any beacon signal. They just passively listen to the broadcasts of the anchor nodes for self-positioning.
4) UPS has low computation overhead. It is based on simple algebraic operations on scalar values.
5) As evidenced by our simulation study, UPS has low position error. It is applicable to both localization and navigation in UWA-SNs.

The silent positioning feature of UPS deserves further emphasis. First, it can significantly conserve bandwidth and, therefore, improve network throughput since sensors/vehicles do not transmit any beacon for positioning purpose. This is particularly true when a large number of vehicles and sensors need to be positioned in a UWA-SN. Second, UPS is applicable to asymmetric UWA-SNs where the transmission from an underwater vehicle or sensor could not reach four or more anchor nodes. Third, silent positioning provides strong location privacy, which can help protect sensors/vehicles from being detected in critical applications.

This paper is organized as follows: Section II summarizes the major related works in UWA-SNs. Section III proposes UPS, i.e., a silent underwater positioning scheme for UWA-SN. Underwater acoustic channel modeling and theoretic performance analysis are given in Section IV. Simulation results are reported in Section V. We conclude our paper and report our future research in Section VI.

II. Related Work

Sensor self-positioning has been extensively studied for typical indoor and outdoor sensor networks [16], [20]. In this section, we briefly overview the localization techniques proposed in UWA-SNs. For a more detailed literature survey, see [15] and the references therein.

Underwater acoustic localization can be broadly classified into two categories: 1) *range-based* and 2) *range-free*. Range-based schemes first measure or estimate distances or angles to a small number of anchor nodes via ToA, RSS, AoA, or even network connectivity and then apply triangulation or multilateration to transform ranges into coordinates. Range-free schemes explore the local topology, and the position estimate is derived from the locations of the surrounding anchor nodes. Generally speaking, range-based schemes have higher position accuracy, whereas range-free schemes provide coarser location estimation.

An area-based range-free underwater positioning (area localization scheme, ALS) is proposed in [14]. ALS relies on the variable power levels of anchor nodes to partition the plan into areas. Each anchor node has its own nonoverlapping partition. A vehicle/sensor receives its position estimate from a central server after providing all the areas (one for each anchor node) where it resides. UPS is a range-based scheme with much higher position accuracy.

Range-based underwater localization requires either long-range or short-range anchors. Since a short-range beacon covers a smaller space, a larger number of anchor nodes are involved; therefore, it is unfavorable in underwater environment. Motivated by terrestrial GPS, *underwater GPS*, such as GPS intelligent buoys (GIBs) [9] and PARADIGM [8], has been proposed. Even though PARADIGM is able to compute location onboard, GIB relies on a centralized server to compute location for underwater vehicles/sensors. These two methods require time synchronization for ToA measurement between anchor nodes and underwater vehicles/sensors. Hahn and Rice [18] propose a ping-pong-style scheme to measure the round-trip delay for range estimation. All these long-range-based methods require underwater vehicles/sensors to interrogate with multiple surface buoys, which contributes to network throughput degradation compared to UPS's silent positioning.

If there is no direct communication between anchor nodes and sensors, network connectivity can be explored for range estimation. In [25], three range detection methods based on network connectivity have been proposed: 1) DV-hop; 2) DV-distance; and 3) Euclidean. A comparison study in [25] indicates that Euclidean performs best in anisotropic topologies with a tradeoff of larger computation and communication overheads. Zhou *et al.* [32] have extended the Euclidean method to 3-D UWA-SN and studied its performance. This method relies on a relatively larger number of anchor nodes, which results in higher deployment cost. Zhang and Cheng [31] propose UR-PLACE, i.e., a protocol for underwater robot self-positioning that exploits the multihop connectivity to anchor nodes via beacon flooding. The extensive local communication in [32] and the global flooding in [31] worsen the bandwidth shortage problem in UWA-SN, which unavoidably degrades the network throughput. As a comparison, our UPS requires no active transmission from underwater vehicles/sensors.

III. UPS: An Underwater Positioning Scheme

In this section, we propose UPS, i.e., a silent acoustic positioning scheme for underwater vehicle/sensor localization. UPS is motivated by our previous work presented for 2-D terrestrial sensor networks [16], [22], [30], which rely on the ToA of RF signals from three anchor nodes for location estimation. The propagation characteristics of RF signals in free space and those of acoustic signals underwater are significantly different,

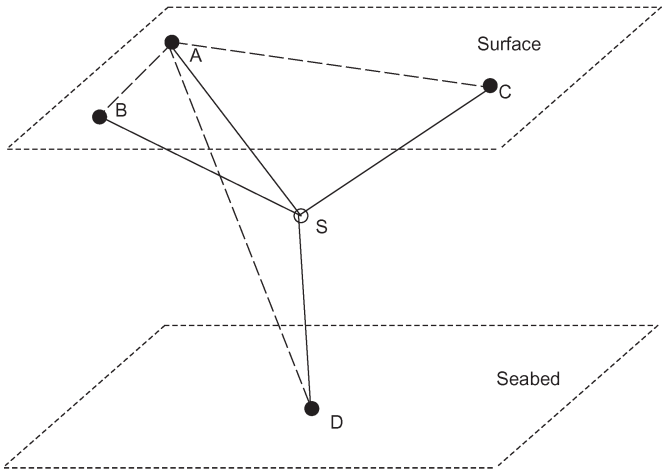

Fig. 1. Sensor S will measure the arrival times of beacon signals from anchor nodes A, B, C, and D locally. S will also receive the turn-around delay information from B, C, and D. B's transmission will start after it receives A's beacon signal. C's transmission will start after it receives the beacon signals of both A and B. In addition, D's transmission will start after it receives the beacon signals of A, B, and C. This procedure will be repeated once every T seconds.

which fundamentally affect the performance of any position algorithm.

UPS consists of two steps: The first step detects the differences of signal arrival times from four anchor nodes. These time differences are transformed into range differences from the underwater vehicle/sensor to the anchor nodes. In the second step, trilateration is performed to transform these range estimates into coordinates. In the following, we first discuss the network model under our consideration.

A. Network Model

We assume that a UWA-SN consists of mobile underwater vehicles (e.g., UUVs or AUVs) and stationary sensors. UUVs and AUVs move about at a typical speed of about 2 m [26] within a confined space, which also covers all nonmobile sensors. To ease our elaboration, hereinafter, we use "sensor" to denote both a mobile vehicle or a stationary sensor. There exist at least four noncospace anchor nodes with long-range beacons, whose locations are known *a priori*. Each of them is equipped with an acoustic transmitter that can cover the whole activity space. No three anchors are collinear. An example layout of anchor nodes is illustrated in Fig. 1.

B. Time-Based Location Detection Scheme

Given the locations (x_a, y_a, z_a), (x_b, y_b, z_b), (x_c, y_c, z_c), and (x_d, y_d, z_d) of anchor nodes A, B, C, and D, respectively, we are going to determine the location (x, y, z) of sensor S, as shown in Fig. 1. Let d_{ij} be the distance between i and j, where $i, j \in \{a, b, c, d, s\}$, representing the four anchor nodes and sensor S. We have

$$d_{ab} = \sqrt{(x_a - x_b)^2 + (y_a - y_b)^2 + (z_a - z_b)^2}$$

$$d_{ac} = \sqrt{(x_a - x_c)^2 + (y_a - y_c)^2 + (z_a - z_c)^2}$$

$$d_{ad} = \sqrt{(x_a - x_d)^2 + (y_a - y_d)^2 + (z_a - z_d)^2}.$$

The first step of UPS computes the range differences between d_{sa} and d_{sb}, d_{sc}, and d_{sd}, respectively.

Step 1—Range Difference Computation: Let A be the master anchor node, which initiates a beacon signal every T seconds. Each beacon interval begins when A transmits a beacon signal. Considering any beacon interval i, at times t_1^i, t_b^i, t_c^i, and t_d^i, sensor S and anchor nodes B, C, and D receive A's beacon signal, respectively. At time $t_b^{i\prime}$, which is $\geq t_b^i$, B replies to A with a beacon signal conveying information $t_b^{i\prime} - t_b^i = \Delta t_b^i$. This signal reaches S at time t_2^i. After receiving beacon signals from both A and B, at time $t_c^{i\prime}$, C replies to A with a beacon signal conveying information $t_c^{i\prime} - t_c^i = \Delta t_c^i$. This signal reaches S at time t_3^i. After receiving beacon signals from A, B, and C, at time $t_d^{i\prime}$, D replies to A with a beacon signal conveying information $t_d^{i\prime} - t_d^i = \Delta t_d^i$. This signal reaches S at time t_4^i. Based on triangle inequality, $t_1^i < t_2^i < t_3^i < t_4^i$. Letting $\Delta t_1^i = t_2^i - t_1^i$, $\Delta t_2^i = t_3^i - t_1^i$, and $\Delta t_3^i = t_4^i - t_1^i$, we obtain

$$d_{ab} + d_{sb} - d_{sa} + v \cdot \Delta t_b^i = v \cdot \Delta t_1^i \quad (1)$$

$$d_{ac} + d_{sc} - d_{sa} + v \cdot \Delta t_c^i = v \cdot \Delta t_2^i \quad (2)$$

$$d_{ad} + d_{sd} - d_{sa} + v \cdot \Delta t_d^i = v \cdot \Delta t_3^i \quad (3)$$

which gives

$$d_{sb} = d_{sa} + v \cdot \Delta t_1^i - d_{ab} - v \cdot \Delta t_b^i = d_{sa} + k_1^i \quad (4)$$

$$d_{sc} = d_{sa} + v \cdot \Delta t_2^i - d_{ac} - v \cdot \Delta t_c^i = d_{sa} + k_2^i \quad (5)$$

$$d_{sd} = d_{sa} + v \cdot \Delta t_3^i - d_{ad} - v \cdot \Delta t_d^i = d_{sa} + k_3^i \quad (6)$$

where d_{sa}, d_{sb}, d_{sc}, and d_{sd} are positive real numbers; v is the speed of the ultrasound; and

$$k_1^i = v \cdot \Delta t_1^i - v \cdot \Delta t_b^i - d_{ab} \quad (7)$$

$$k_2^i = v \cdot \Delta t_2^i - v \cdot \Delta t_c^i - d_{ac} \quad (8)$$

$$k_3^i = v \cdot \Delta t_3^i - v \cdot \Delta t_d^i - d_{ad}. \quad (9)$$

Averaging k_1^i, k_2^i, and k_3^i over I intervals gives

$$k_1 = \frac{v}{I}\left[\sum_{i=1}^{I}\left(\Delta t_1^i - \Delta t_b^i\right)\right] - d_{ab} \quad (10)$$

$$k_2 = \frac{v}{I}\left[\sum_{i=1}^{I}\left(\Delta t_2^i - \Delta t_c^i\right)\right] - d_{ac} \quad (11)$$

$$k_3 = \frac{v}{I}\left[\sum_{i=1}^{I}\left(\Delta t_3^i - \Delta t_d^i\right)\right] - d_{ad}. \quad (12)$$

We are going to apply trilateration with k_1, k_2, and k_3 to compute coordinates (x, y, z) for sensor S in the next step.

Remarks:

1) All arrival times, including t_j^i, where $j = 1, 2, 3, 4$, and $t_j^{i\prime}$, where $j \in \{b, c, d\}$, are based on the local timers of the anchor nodes and sensor S. No time synchronization is required.
2) We require A to periodically initiate the beacon signal transmission to decrease the measurement error and to facilitate navigation.

Step 2—Location Computation: From (4)–(6) and (10)–(12), we have

$$d_{sb} = d_{sa} + k_1 \tag{13}$$

$$d_{sc} = d_{sa} + k_2 \tag{14}$$

$$d_{sd} = d_{sa} + k_3. \tag{15}$$

Based on trilateration, we obtain four equations with four unknowns x, y, z, and d_{sa}, where $d_{sa} > 0$, i.e.,

$$(x - x_a)^2 + (y - y_a)^2 + (z - z_a)^2 = d_{sa}^2 \tag{16}$$

$$(x - x_b)^2 + (y - y_b)^2 + (z - z_b)^2 = (d_{sa} + k_1)^2 \tag{17}$$

$$(x - x_c)^2 + (y - y_c)^2 + (z - z_c)^2 = (d_{sa} + k_2)^2 \tag{18}$$

$$(x - x_d)^2 + (y - y_d)^2 + (z - z_d)^2 = (d_{sa} + k_3)^2. \tag{19}$$

Without loss of generality, we assume that the four anchor nodes are located at (0, 0, 0), $(x_b, 0, 0)$, $(x_c, y_c, 0)$, and (x_d, y_d, z_d), respectively, where $x_b > 0$, $y_c > 0$, and $z_d > 0$. Note that we can always transform real positions to this coordinate system through rotation and translation.

From (16)–(19), we have

$$x^2 + y^2 + z^2 = d_{sa}^2 \tag{20}$$

$$(x - x_b)^2 + y^2 + z^2 = (d_{sa} + k_1)^2 \tag{21}$$

$$(x - x_c)^2 + (y - y_c)^2 + z^2 = (d_{sa} + k_2)^2 \tag{22}$$

$$(x - x_d)^2 + (y - y_d)^2 + (z - z_d)^2 = (d_{sa} + k_3)^2. \tag{23}$$

Solving these equations, we obtain

$$d_{sa}^{(1)} = \frac{-\beta - \sqrt{\beta^2 - 4\alpha\gamma}}{2\alpha} \tag{24}$$

$$d_{sa}^{(2)} = \frac{-\beta + \sqrt{\beta^2 - 4\alpha\gamma}}{2\alpha} \tag{25}$$

$$x = A_x d_{sa} + B_y \tag{26}$$

$$y = A_y d_{sa} + B_y \tag{27}$$

$$z = A_z d_{sa} + B_z \tag{28}$$

where

$$\alpha = A_x^2 + A_y^2 + A_z^2 - 1 \tag{29}$$

$$\beta = 2(A_x B_x + A_y B_y + A_z B_z) \tag{30}$$

$$\gamma = B_x^2 + B_y^2 + B_z^2 \tag{31}$$

$$A_x = -\frac{k_1}{x_b} \tag{32}$$

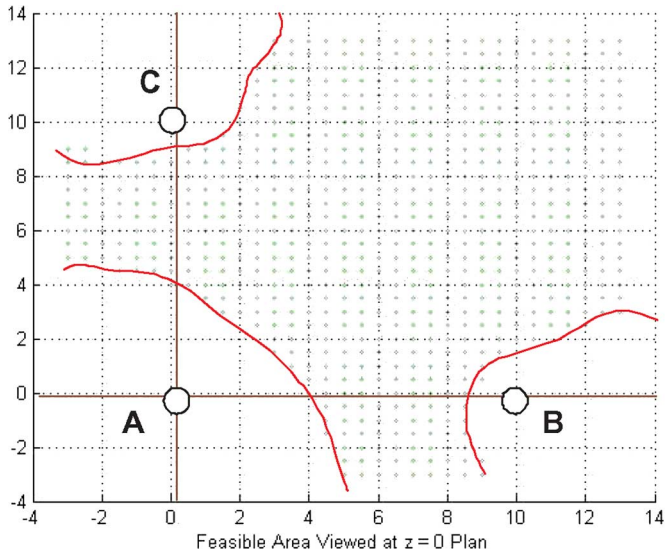

Fig. 2. Transection of the feasible space where $z = 0$.

$$B_x = \frac{x_b^2 - k_1^2}{2x_b} \tag{33}$$

$$A_y = \frac{k_1 x_c}{x_b y_c} - \frac{k_2}{y_c} \tag{34}$$

$$B_y = \frac{x_c^2 + y_c^2 - x_b x_c + \frac{x_c k_1^2}{x_b} - k_2^2}{2y_c} \tag{35}$$

$$A_z = \frac{k_1 x_d}{x_b z_d} - \frac{k_3}{z_d} - \frac{y_d\left(\frac{k_1 x_c}{x_b} - k_2\right)}{y_c z_d} \tag{36}$$

$$B_z = \frac{x_d^2 + y_d^2 + z_d^2 - x_b x_d + \frac{x_d k_1^2}{x_b} - k_3^2 - \frac{y_d x_c^2}{y_c}}{2z_d} + \frac{-y_c y_d + \frac{x_b x_c y_d}{y_c} - \frac{k_1^2 x_c y_d}{x_b y_c} + \frac{k_2^2 y_d}{y_c}}{2z_d}. \tag{37}$$

We have conducted extensive simulation to study the *feasible space* where $d_{sa} > 0$ is unique. It is interesting to observe that when S is not close to any anchor node and when it is not behind any anchor node, (24) provides a unique feasible solution. In addition, the correct position can be computed via (24) if a sensor resides in the enclosed space by the four anchor nodes, even when it is close to an anchor node. Figs. 2–4 report the three transections $(z = 0, 5, 10)$ of the feasible space (the gray area) when the four anchor nodes A, B, C, and D reside in (0, 0, 0), (10, 0, 0), (0, 10, 0), and (0, 0, 10), respectively.

IV. Channel Modeling and Theoretical Performance Analysis

In this section, we study the position error of UPS that resulted from the acoustic fading channel. In the following, we first propose a modified UWB S-V model to characterize the underwater acoustic fading channel; then, we apply this model to study the position error of UPS. Major sources of position errors are also identified. Note that, to the best of our

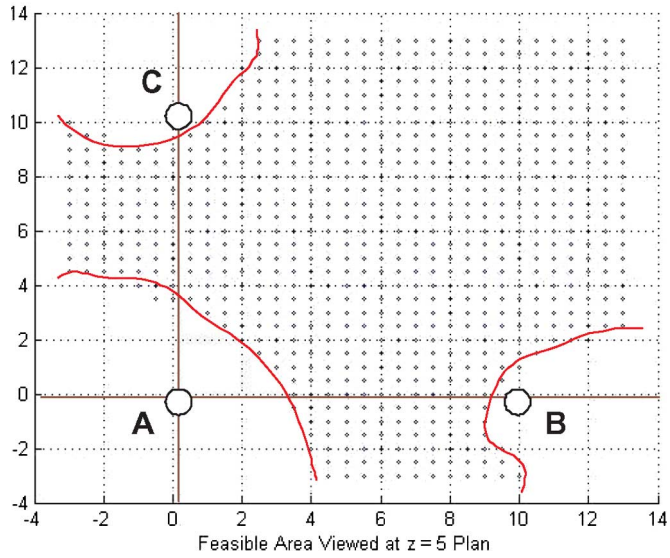

Fig. 3. Transection of the feasible space where $z = 5$.

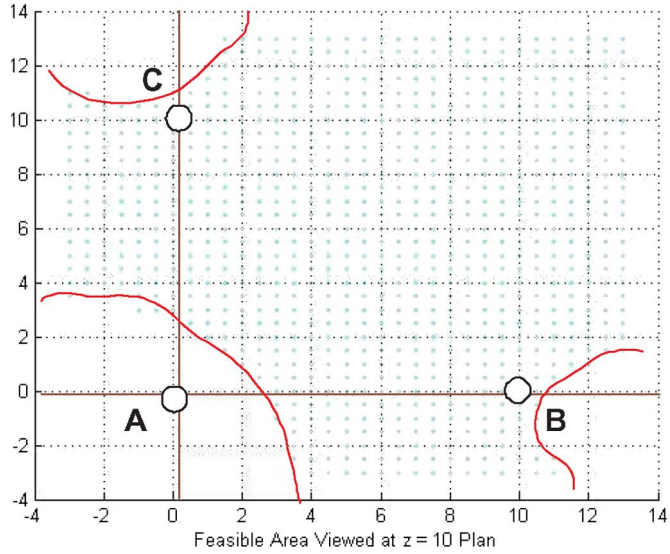

Fig. 4. Transection of the feasible space where $z = 10$.

knowledge, there is no standard channel model for underwater so far, and our modified UWB S-V model is a reasonable model based on the study on outdoor UWB channel detailed in [21].

A. Channel Modeling for Underwater Sensor Networks

The underwater acoustic channel exhibits phenomena such as signal fading and phase and amplitude fluctuation due to the interactions with the boundaries and the scattering from inhomogeneities within the ocean medium. The speed of sound underwater is approximately 1500 m/s, which leads to large propagation delays and motion-induced Doppler effects. Phase and amplitude fluctuations may induce high bit-error probability, compared to most radio channels. Multipath interference is another important phenomena in UWA networks, causing frequency-selective fading in underwater channels.

There has been much effort to model the underwater acoustic fading channels and estimate their performance. Early research [13], [28] assumes Rayleigh fading in nature, but it is later observed in [17] that Rayleigh fading exhibits only in limited cases. Geng and Zielinski [17] propose that, in an underwater acoustic channel, there can be several distinct paths (eigenpaths) over which a signal can propagate from transmitter to receiver (eigenpath signals). Each eigenpath signal contains a dominant stable component and many smaller randomly scattered components (sub-eigenpath or eigenray components). The envelope of the eigenpath signal can therefore be described using a Rice fading model. Such an *eigenpath or eigenray* concept was first introduced in [19]. The eigenray arrival angles, as well as the amplitude and phase fluctuations, are all statistically modeled and are assumed to be independent of each other. The number of eigenrays reaching the receiver is a Poisson distribution with a mean number calculated from the Ray Theory.

Enlightened by the prior research on underwater acoustic channel modeling, we propose a modified UWB S-V channel model [27] for underwater acoustic networks, which can be validated in three considerations: First, UWB comes from the UWB radar world and refers to the electromagnetic waveforms that are characterized by an instantaneous fractional energy bandwidth greater than about 0.20–0.25. In an underwater acoustic channel, the communication frequency range is inferior to 10 kHz. In short-range transmission, the carrier frequency is 550 Hz in shallow water and 2 kHz in deep water. The carrier frequency for long-range transmission is 1500 Hz. In all cases, the fractional bandwidth $(f_H - f_L)/((f_H + f_L)/2)$ is much greater than 0.20–0.25. Therefore, the underwater acoustic channel can be modeled as a UWB channel. In July 2003, the Channel Modeling subcommittee of study group IEEE 802.15.SG3a published the final report regarding the UWB indoor multipath channel model [2]. It is a modified version of the indoor S-V channel model [27]. Second, multipath channels can be modeled as an S-V model in UWB communications. The S-V model is based on the observation that, usually, multipath contributions generated by the same pulse arrive at the receiver grouped into clusters. Such a channel behavior is analogous to the aforementioned eigenpath/sub-eigenpath concept in underwater networks. Third, similar to [19], two Poisson models are employed in the modeling of the path arrivals in UWB communications. The first Poisson model is for the first path of each path cluster, and the second Poisson model is for the paths or rays within each cluster.

Applying the S-V model into underwater acoustic channels, the arrival of clusters is modeled as a Poisson arrival process with rate Λ, whereas, within each cluster, subsequent multipath contributions or rays also arrive according to a Poisson process with rate λ (see Fig. 5). We define the following.

- T_l is the arrival time of the first path of the lth cluster.
- $\tau_{k,l}$ is the delay of the kth path within the lth cluster relative to the first path arrival time T_l.
- Λ is the cluster arrival rate.
- λ is the ray arrival rate, i.e., the arrival rate of the paths within each cluster.

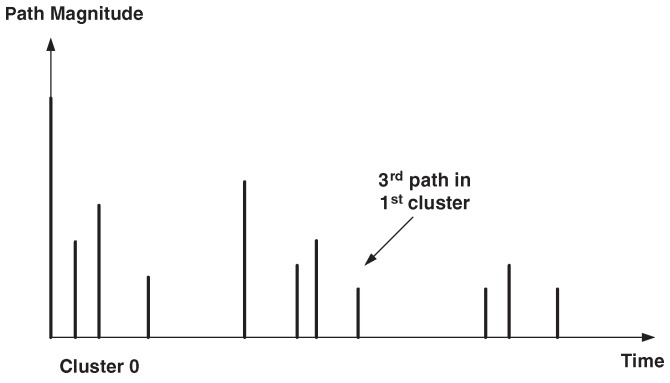

Fig. 5. Channel impulse response.

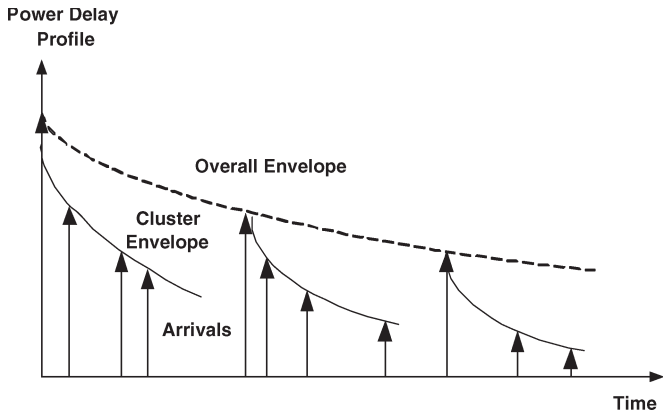

Fig. 6. Double exponential decay of the mean cluster power and the ray power within clusters.

By definition, we have $\tau_{0l} = T_l$. The distributions of the cluster arrival time and the ray arrival time are given by

$$p(T_l|T_{l-1}) = \Lambda \exp(-\Lambda(T_l - T_{l-1}), \qquad l > 0$$
$$p\left(\tau_{k,l}|\tau_{(k-1),l}\right) = \lambda \exp\left(-\lambda\left(\tau_{k,l} - \tau_{(k-1),l}\right)\right), \qquad k > 0. \tag{38}$$

In the UWB S-V model, the magnitude of the kth path within the lth cluster is denoted by β_{kl}. It follows a Rayleigh distribution. However, in underwater acoustic networks, the channel within the communication frequency range does not behave like a Rayleigh channel. Based on the discussion in [17] and [19], it is rather appropriate to model the multipath channel gain as a Rician distribution. Then, in the underwater S-V model, the gain of the kth path within the lth cluster is a complex random value with a modulus β_{kl} and a phase θ_{kl}. We assume that the β_{kl} values in a underwater acoustic channel are statistically independent and are Rician-distributed positive random variables, whereas the θ_{kl} values are assumed to be statistically independent uniform random variables over $[0, 2\pi)$. We have

$$\overline{\beta_{kl}^2} = \overline{\beta_{00}^2} \exp(-T_l/\Gamma) \exp(-\tau_{kl}/\gamma) \tag{39}$$

where the term β_{00} represents the average energy of the first path of the first cluster, whereas Γ and γ are the power decay coefficients for clusters and multipath, respectively. According to (39), the average power decay profile is characterized by an exponential decay of the amplitude of the clusters and a different exponential decay for the amplitude of the received pulses within each cluster, as shown in Fig. 6.

In [23], based on many experimentations carried out by Loubet and Faure with the French Navy, it was shown that the Rayleigh fading model is not fit for underwater transmissions. They proposed the underwater channel model using ray tracing by great deterministic propagation paths (macromultipath) associated with random fluctuations (micromultipaths). The macromultipaths are very similar to the clusters in our model, and the micromultipaths are very similar to the rays within each cluster in our model.

B. Theoretical Error Analysis

In this section, we study the position error of S that resulted from the acoustic fading channel, which has been modeled as a modified UWB S-V model in Section IV-A.

The trilateration equations (16)–(19) compute the coordinates (x, y, z) for sensor S based on the measured values k_1, k_2, and k_3, which are determined by the time-related measurements at the sensor (Δt_1^i, Δt_2^i, and Δt_3^i) and anchor nodes B (Δt_b^i), C (Δt_c^i), and D (Δt_d^i) over beacon interval i [see (10)–(12)]. Therefore, the errors of x, y, and z result from the measuring errors of Δt_1^i, Δt_2^i, Δt_3^i, Δt_b^i, Δt_c^i, and Δt_d^i. Since the error of Δt_b^i ($\Delta t_c^i, \Delta t_d^i$) plays the same role as that of Δt_1^i ($\Delta t_2^i, \Delta t_3^i$) in the computation of k_1 (k_2, k_3) and anchor node B (C, D) and can have more sophisticated hardware to precisely estimate Δt_b^i ($\Delta t_c^i, \Delta t_d^i$), we consider the errors of Δt_1^i, Δt_2^i, and Δt_3^i only, which are computed from the arrival times of the beacon signals transmitted from anchor nodes A, B, C, and D at beacon internal i t_1^i, t_2^i, t_3^i, and t_4^i, respectively.

Assume that the underwater sensor always listens to the first ray of the transmitted signal and records the arrival times, which, in our case, are t_1^i, t_2^i, t_3^i, and t_4^i. Due to the underwater multipath effect, as illustrated in Fig. 6, these arrival times contain an error with an exponential distribution. Let $\delta_{t_1}^i$, $\delta_{t_2}^i$, and $\delta_{t_3}^i$ be the measuring errors of Δt_1^i, Δt_2^i, and Δt_3^i, respectively. It is reasonable to assume that $\delta_{t_1}^i$, $\delta_{t_2}^i$, and $\delta_{t_3}^i$ are independent from each other. Given t_1^i, the conditional probability density functions of $\delta_{t_1}^i$, $\delta_{t_2}^i$, and $\delta_{t_3}^i$ are exponential with parameters λ_1, λ_2, and λ_3, respectively, i.e.,

$$\begin{aligned} P_e\left(\delta_{t_1}^i|t_1^i\right) &= \lambda_1 \exp\left(-\lambda_1 \delta_{t_1}^i\right) \\ P_e\left(\delta_{t_2}^i|t_1^i\right) &= \lambda_2 \exp\left(-\lambda_2 \delta_{t_2}^i\right) \\ P_e\left(\delta_{t_3}^i|t_1^i\right) &= \lambda_3 \exp\left(-\lambda_3 \delta_{t_3}^i\right). \end{aligned} \tag{40}$$

To simplify the elaboration, we consider the case when anchor nodes A, B, C, and D are located at (0, 0, 0), (R, 0, 0), (0, R, 0), and (0, 0, R), respectively. To further simplify the analysis, we consider the case when S resides in a small area (with a diameter $\ll R$) whose center is equidistant to all anchor nodes. The general case can be similarly analyzed.

From (10)–(12), k_1, k_2, and k_3 are the averaged results over I beacon intervals, and based on the central limit theorem, k_1, k_2, and k_3 are approximately normally distributed when I is large. Therefore, we may assume that k_1, k_2, and k_3 are distributed according to $\mathcal{N}(\mu_1, \sigma_1^2)$, $\mathcal{N}(\mu_2, \sigma_2^2)$, and $\mathcal{N}(\mu_3, \sigma_3^2)$, respectively. Deducing from (10)–(12), we have

$$\begin{aligned} k_1 : \mu_1 &= v\left(\frac{1}{\lambda_1} + \nu_1\right) - R, \qquad \sigma_1^2 = \frac{v^2}{I\lambda_1^2} \\ k_2 : \mu_2 &= v\left(\frac{1}{\lambda_2} + \nu_2\right) - R, \qquad \sigma_2^2 = \frac{v^2}{I\lambda_2^2} \\ k_3 : \mu_3 &= v\left(\frac{1}{\lambda_3} + \nu_3\right) - R, \qquad \sigma_3^2 = \frac{v^3}{I\lambda_3^2} \end{aligned} \tag{41}$$

where ν_1, ν_2, and ν_3 are the mean of the accurate values for Δt_1^i, Δt_2^i, and Δt_3^i, respectively.

Based on these assumptions, we have $\mu_1/R \approx 0$, $\mu_2/R \approx 0$, and $\mu_3/R \approx 0$. Plugging $x_b = y_c = z_d = R$ and other zero coordinates into (24) and simplifying its solution by approximating k_1^2/R^2, k_2^2/R^2, and k_3^2/R^2 with 0, we end up with

$$d_{sa} \approx \frac{\sqrt{3R^2 + (k_1 + k_2 + k_3)^2} - (k_1 + k_2 + k_3)}{2}. \tag{42}$$

Substituting the preceding equation into (26) yields

$$x \approx \frac{R}{2} - \frac{k_1^2}{2R} - \frac{k_1}{R}\frac{\sqrt{3R^2 + (k_1+k_2+k_3)^2} - (k_1+k_2+k_3)}{2}. \tag{43}$$

Now, replacing $(k_1k_2/R^2) = (k_1/R)(k_2/R)$, $(k_1k_3/R^2) = (k_1/R)(k_3/R)$, and $(k_2k_3/R^2) = (k_2/R)(k_3/R)$ by 0, we obtain

$$x \approx \frac{R}{2} + \frac{k_1}{2R}(k_2 + k_3) - k_1\sqrt{\frac{3}{2}} = \frac{R}{2} + k_1 k_{2,3}^* \tag{44}$$

where $k_{2,3}^* = (k_2 + k_3)/2R - \sqrt{3/2}$. Similarly, from (27) and (28), we have

$$\begin{aligned} y &\approx \frac{R}{2} + \frac{k_2}{2R}(k_1 + k_3) - k_2\sqrt{\frac{3}{2}} = \frac{R}{2} + k_2 k_{1,3}^* \\ z &\approx \frac{R}{2} + \frac{k_3}{2R}(k_1 + k_2) - k_3\sqrt{\frac{3}{2}} = \frac{R}{2} + k_3 k_{1,2}^* \end{aligned} \tag{45}$$

where $k_{1,3}^* = (k_1 + k_3)/2R - \sqrt{3/2}$, and $k_{1,2}^* = (k_1 + k_2)/2R - \sqrt{3/2}$.

Since (x, y, z) is used to estimate the location of S, the error in the estimation must be addressed. There are several ways to do this. The following is a common practice, where the variance of each variable is computed, and the size of the variance or standard deviation is used as a measure of the estimation error.

As k_1 has a Gaussian distribution with mean μ_1 and variance σ_1^2, k_2 has a Gaussian distribution with mean μ_2 and variance σ_2^2, and k_3 has a Gaussian distribution with mean μ_3 and variance σ_3^2, the linear combination $k_{1,3}^*$ has a Gaussian distribution with mean $(\mu_1 + \mu_3)/2R - \sqrt{3/2}$ and variance $(\sigma_1^2 + \sigma_3^2)/4R^2$, $k_{1,2}^*$ has a Gaussian distribution with mean $(\mu_1 + \mu_2)/2R - \sqrt{3/2}$ and variance $(\sigma_1^2 + \sigma_2^2)/4R^2$, and $k_{2,3}^*$ has a Gaussian distribution with mean $(\mu_2 + \mu_3)/2R - \sqrt{3/2}$ and variance $(\sigma_2^2 + \sigma_3^2)/4R^2$. Denote by $E(X)$ and $V(X)$ the mean and variance of random variable X. We have, from (44)

$$\begin{aligned} V(x) &\approx V\left(k_1 k_{2,3}^*\right) \\ &= E\left(k_1 k_{2,3}^*\right)^2 - \left[E\left(k_1 k_{2,3}^*\right)\right]^2 \\ &= E\left(k_1^2\left(k_{2,3}^*\right)^2\right) - \left[E\left(k_1 k_{2,3}^*\right)\right]^2. \end{aligned} \tag{46}$$

By the independence between k_1, k_2, and k_3, we have

$$E\left(k_1 k_{2,3}^*\right) = E(k_1)E\left(k_{2,3}^*\right) \tag{47}$$

$$\begin{aligned} E\left(k_1^2\left(k_{2,3}^*\right)^2\right) &= E\left(k_1^2\right)E\left(k_{2,3}{}^{*2}\right) \\ &= \left[V(k_1) + (E(k_1))^2\right] \\ &\quad \times \left[V\left(k_{2,3}^*\right) + \left(E\left(k_{2,3}^*\right)\right)^2\right]. \end{aligned} \tag{48}$$

Therefore, substitution gives

$$\begin{aligned} V(x) &\approx V(k_1)\left[E\left(k_{2,3}^*\right)\right]^2 + V\left(k_{2,3}^*\right)\left[E(k_1)\right]^2 \\ &\quad + V(k_1)V\left(k_{2,3}^*\right) \\ &= \sigma_1^2\left(\frac{\mu_2 + \mu_3}{2R} - \sqrt{\frac{3}{2}}\right)^2 + \frac{\sigma_2^2 + \sigma_3^2}{4R^2}\mu_1^2 + \sigma_1^2\frac{\sigma_2^2 + \sigma_3^2}{4R^2} \\ &= \frac{\sigma_1^2(\mu_2 + \mu_3)^2 + \left(\sigma_2^2 + \sigma_3^2\right)\mu_1^2 + \sigma_1^2\left(\sigma_2^2 + \sigma_3^2\right)}{4R^2} \\ &\quad + \sigma_1^2\left(\frac{3}{2} - \frac{\mu_2 + \mu_3}{R}\sqrt{\frac{3}{2}}\right). \end{aligned} \tag{49}$$

Since $\mu_1/R \approx 0$ and $\mu_2/R \approx 0$, plugging in (42), the preceding equation reduces to

$$\begin{aligned} V(x) &\approx \frac{\sigma_1^2}{2}\left(3 + \frac{\sigma_2^2 + \sigma_3^2}{2R^2}\right) \\ &= \frac{v^2}{2I\lambda_1^2}\left[3 + \frac{v^2}{2IR\left(\lambda_2^2 + \lambda_3^2\right)}\right]. \end{aligned} \tag{50}$$

Similarly, we have

$$\begin{aligned} V(y) &\approx V\left(k_{1,3}^*\right)\left[E(k_2)\right]^2 + V(k_2)\left[E\left(k_{1,3}^*\right)\right]^2 \\ &\quad + V\left(k_{1,3}^*\right)V(k_2) \\ &\approx \frac{\sigma_2^2}{2}\left(3 + \frac{\sigma_1^2+\sigma_3^2}{2R^2}\right) \\ &= \frac{v^2}{2I\lambda_2^2}\left[3 + \frac{v^2}{2IR\left(\lambda_1^2+\lambda_3^2\right)}\right]. \end{aligned} \tag{51}$$

$$\begin{aligned} V(z) &\approx V\left(k_{1,2}^*\right)\left[E(k_3)\right]^2 + V(k_3)\left[E\left(k_{1,2}^*\right)\right]^2 \\ &\quad + V\left(k_{1,2}^*\right)V(k_3) \\ &\approx \frac{\sigma_3^2}{2}\left(3 + \frac{\sigma_1^2+\sigma_2^2}{2R^2}\right) \\ &= \frac{v^2}{2I\lambda_3^2}\left[3 + \frac{v^2}{2IR\left(\lambda_1^2+\lambda_2^2\right)}\right]. \end{aligned} \tag{52}$$

From the preceding analysis, we make the following observations: First, the variances of x, y, and z depend on ray arrival rates λ_1, λ_2, and λ_3. Second, λ_1 contributes more to the variance of x than λ_2 and λ_3, λ_2 contributes more to the variance of y than λ_1 and λ_3, and λ_3 contributes more to the variance of z than λ_1 and λ_2. Third, when R is large, $V(x) \approx 3\sigma_1^2/2 = 3v^2/2I\lambda_1^2$, $V(y) \approx 3\sigma_2^2/2 = 3v^2/2I\lambda_2^2$, and $V(z) \approx 3\sigma_3^2/2 = 3v^2/2I\lambda_3^2$, showing that the variance of x is dependent on that of k_1, the variance of y is dependent on that of k_2, and the variance of z is dependent on that of k_3. Fourth, if $\lambda_1 = \lambda_2 = \lambda_3$, the variances of x, y, and z can be treated the same in practice.

Note that the preceding analysis well explains our simulation results, which indicate that position errors strongly depend on the arrival rates of double exponential distributions.

C. Sources of Errors

There are three major sources of errors for time-based location detection schemes in UWA-SNs: 1) *the receiver system delay*; 2) *the underwater multipath fading*; and 3) *the variable acoustic speed underwater*. The receiver system delay is the time duration from which the signal hits the receiver antenna until the signal is accurately decoded by the receiver. This time delay is determined by the receiver electronics. Usually, it is constant or varies in very small scale when the receiver and the channel are free from interference. This system delay can be predetermined and used to calibrate the measurements. For example, anchor nodes B, C, and D can always eliminate the system delay from Δt_b^i, Δt_c^i, and Δt_d^i before these values are conveyed to the sensors in their reply messages to A's beacon signal. Meanwhile, as Δt_1^i, Δt_2^i, and Δt_3^2 are measured by one sensor, the effect of receiver system delay may cancel out. Thus, in our model, if anchor nodes B, C, and D can provide precise *a priori* information on receiver system time delays, the effect of these delays will be negligible.

The underwater multipath fading channel will greatly influence the location accuracy of any location detection system. Major factors influencing terrestrial multipath fading [6] include *multipath propagation*, *speed of the receiver*, *speed of the surrounding objects*, and the *transmission signal bandwidth*. In the underwater environment, other important factors include *water temperature and clarity*, *motion behavior of receiver and underwater objects*, and *transmission range*. In our time-based location scheme, we assume that the motion of the underwater vehicles is relatively small such that the motion-induced Doppler effect can be ignored.

There are two important characteristics of multipath signals: First, the multiple nondirect path signals will always arrive at the receiver antennas later than the direct path signal, as they must travel a longer distance. Second, in the line-of-sight transmission model, nondirect multipath signals will normally be weaker than the direct path signal, as some signal power will be lost from scattering. If nonline-of-sight exists, the nondirect multipath signal may be stronger, as the direct path is hindered in some way. Based on these characteristics, scientists can always design more sensitive receivers to lock and track the direct path signal. For example, multipath signals using a pseudorandom code arriving at the receiver later than the direct path signal will have negligible effects on a high-resolution direct-sequence binary phase-shift keying receiver [11]. Our location detection scheme mitigates the effect of multipath fading by measuring TDoA over multiple beacon intervals and modeling the multipath arrival times as the double exponential distribution. TDoA measurements have been very effective in fading channels, as many detrimental effects caused by multipath fading and processing delay can be canceled [12].

Another source of position error is the variable speed of sound, which significantly affects the precision of all localization systems that assume a constant acoustic speed. The velocity of underwater acoustics depends on temperature, salinity, and depth [4]. In future research, we will investigate the influence of the variable speed of sound on our positioning scheme.

V. Simulation

In this section, we are going to study the performance of UPS in UWA-SNs. We make the same assumptions as those in Section IV-B; for a given t_1^i, the measuring errors of Δt_i^i, Δt_2^i, and Δt_3^i are independent exponential distributions with arrival rates λ_1, λ_2, and λ_3, respectively, and the underwater vehicle/sensor measures the arrival time of the first ray of the first cluster only in a multipath fading channel. We further assume that the measuring errors of Δt_b^i, Δt_c^i, and Δt_d^i are negligible, as justified in Section IV-C. Therefore, λ_1, λ_2, and λ_3 can be assumed to be equal, and this value is denoted by λ. We will investigate the influence of λ on position error. Another factor that we will investigate is the number of beacon intervals I used to compute k_1, k_2, and k_3. Since we also consider the localization of mobile underwater vehicles, we choose to average over a small number of beacon intervals.

We use Matlab to code UPS. This tool provides procedures to generate normally distributed and uniformly distributed random numbers. Note that we do not use the $sqrt$ function in Matlab. Instead, we use Newton's method [3]. We have found that four

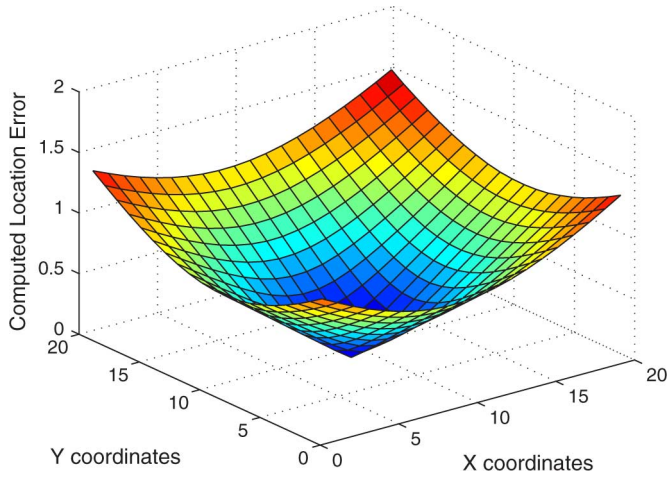

Fig. 7. Position errors versus real positions when $\lambda = 0.1$ in the $x = y$ plane with $z = 5$.

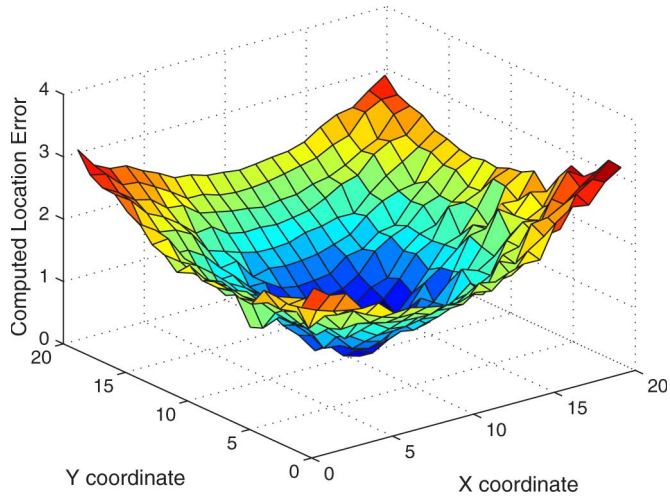

Fig. 8. Position errors versus real positions when $\lambda = 2.5$ in the $x = y$ plane with $z = 5$.

iterations generally yield good results. In addition, (24) will be adopted for position estimation since, in our simulation, sensors will be placed within the space enclosed by four anchor nodes.

First, we study the distribution of position errors over a 3-D monitored space. In this simulation scenario, the four anchor nodes are located at (0, 0, 0), (20, 0, 0), (0, 20, 0), and (0, 0, 20), respectively. Sensors are placed at grid points $(i + 0.5, j + 0.5, k + 0.5)$, where $i, j, k = 0, 1, \ldots, 19$. The errors of Δt_1^i, Δt_2^i, and Δt_3^i are exponentially distributed with parameters $\lambda_1 = \lambda_2 = \lambda_3 = \lambda$. We average the sensor location estimation over 1000 trials. For each trial, $I = 16$. In addition, we simulate different λ settings and obtain similar results. Nevertheless, we report the cases of $\lambda = 0.1$ and $\lambda = 2.5$ only in this paper. Figs. 7 and 8 illustrate the $x = y$ plane position errors versus the real positions of the sensors for $z = 5$. Results from the $x = z$ and $y = z$ planes are close to those reported for the $x = y$ plane.

We observe that a lower arrival rate gives a better estimation since a higher arrival rate may bring motion-induced Doppler shift in the channel and cause jittering in the measurement. We also observe that, as the distances from a sensor to all four anchor nodes become larger, the position errors will

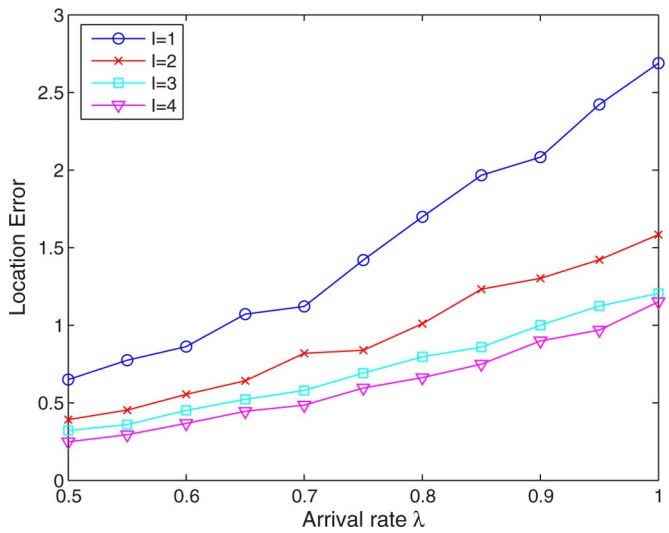

Fig. 9. Position errors versus λ where $\angle BAC = 90°$.

correspondingly become larger; when the sensor is closer to any of the four anchor nodes, the errors become larger. Notice that, in Fig. 7, the sensor at location (9.5, 9.5, 5.0), which is close to the intersection of the three angle bisectors of ΔABC, has the smallest position error and that the sensors at its neighboring area also demonstrate quite low position errors. Interestingly, Bulusu *et al.* [10], Cheng *et al.* [16], and Nasipuri and Li [24] provide similar results in their simulation study. Intuitively, this is because the geometry of the intersection of the range circles is poor when the sensors are far away from any anchor node or when the sensors are close to any anchor node. From this analysis, we conclude that the position error is related to the placement of anchor nodes. Careful studies will be conducted in the future as the results can be applied to guide the deployment of anchor nodes for better performance. For these reasons, in the following simulation, we intentionally enforce an allowable shortest distance (1.0 unit) from any randomly generated sensor to any anchor node. This means that the four anchor nodes are placed some distance away from the boundary of the monitored area.

Next, we consider the scenario when sensors are randomly deployed in a cubic space with lower left corner (1, 1, 1) and upper right corner (19, 19, 19). The four anchor nodes are still located at (0, 0, 0), (20, 0, 0), (0, 20, 0), and (0, 0, 20), respectively. For each λ value, we try 2000 random sensor positions. The averaged results are reported in Fig. 9. Note that, in this paper, I is selected from $\{1, 2, 3, 4\}$ to demonstrate the effectiveness of UPS when applied to positioning mobile underwater vehicles.

We obtain three observations from Fig. 9: First, as I increases, position error decreases. This is because averaging over a larger number of beacon intervals to compute $k_1 k_2$ and k_3 can better smooth out the effects of measuring errors in Δt_1^i, Δt_2^i, and Δt_3^i and, thus, produce an improved result. A detailed theoretical explanation comes from Section IV-B. As I increases, σ_1^2, σ_2^2, and σ_3^2 will decrease, and thus, $V(x)$, $V(y)$ and $V(z)$ will decrease. Then, the errors from estimating the coordinates of sensors by x, y, and z will decrease, implying that the position error will become smaller. Second, position

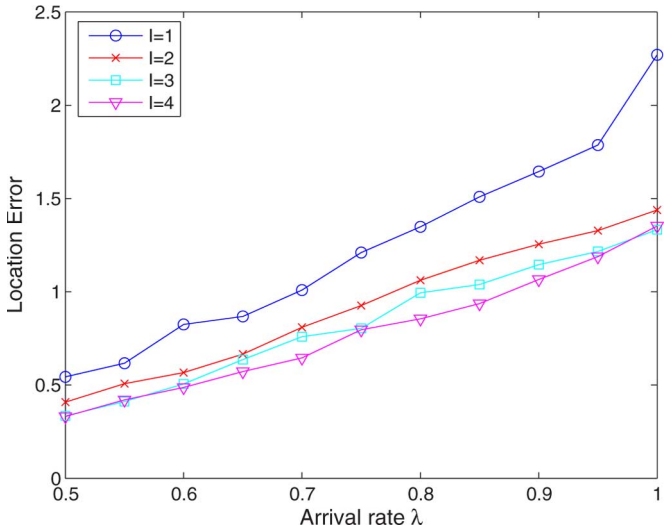

Fig. 10. Position errors versus λ where $\angle BAC \leq 90°$.

error increases as λ increases. This is reasonable in the underwater acoustic channel, in which a higher λ comes from an even higher transmission rate when asymmetry commonly exists between the transmitter and the receiver. Such a characteristic of the underwater medium brings significant multipath interference at the receiver and causes jittering, as shown in Fig. 8. Again, this can be well explained by Section IV-B. In fact, if λ increases, which means that v increases at an even larger pace, v^2/λ^2 increases. As a result, $V(x)$, $V(y)$, and $V(z)$ increase, so that the errors from estimating the coordinates of the sensor by x, y, and z increase. Thus, the larger the arrival rate, the larger the position error. Third, in the situation of small λ, e.g., $\lambda \approx 0.5$, as shown in Fig. 9, the location errors vary very little with the number of beacon intervals I. When λ is relatively high, I plays a more important role. The higher the λ, the bigger the difference induced from I. This observation is analogous to the terrestrial wireless communication channels, in which *coherent time* is introduced to depict a period of time where the channel behavior or model can be considered as stationary. For underwater wireless communications, not only temporal coherence but also spatial and frequency coherences [19] are significant parameters for signal propagation through acoustic channels with multiple paths. Based on the third observation, λ in underwater communications should not be neglected in estimating the coherence parameters. Note that, by rotating the square-cube monitored space within the open space formed by anchor nodes A, B, C, and D, we obtain very similar results.

In the following, we report the simulation results when $\angle BAC \leq 90°$. In this simulation, the four anchor nodes are located at (0, 0, 0), $(X_B, Y_B, 0)$, $(X_C, Y_C, 0)$, and (0, 0, Z_D), respectively, where X_B, Y_B, X_C, Y_C, and Z_D are randomly drawn from [5, 20]. Two thousand sensors are randomly placed within the overlapping space formed by the anchor nodes (A, B, C, D) and the cube space with corners (0, 0, 0) and (20, 20, 20). Fig. 10 reports the position error versus λ. Note that the observations from Fig. 10 are very similar to those from Fig. 9. Nevertheless, for the same λ, the acute angle case performs slightly better than the right angle case.

VI. Conclusion and Future Research

In this paper, we propose UPS, a silent underwater positioning scheme for UWA-SNs. UPS is superior to existing systems in many aspects, such as lack of synchronization and low computation overhead. To evaluate the performance of UPS, we model the underwater acoustic channel with a modified UWB S-V model and conduct both theoretical analysis and a simulation study. Our scheme is simple and effective.

For future research, we will study the impact of the channel modeling error on the position error of UPS. In addition, we intend to design a general framework based on projection such that localization algorithms proposed for 2-D terrestrial sensor networks can be easily tailored to 3-D UWA-SNs. By this approach, the anchor node at the seabed is expected to be saved.

References

[1] *Global Positioning System Standard—Positioning Service Specification*, Jun. 2, 1995.
[2] IEEE 802.15.SG3a, *Channel Modeling Sub-Committee Report Final*, Feb. 2003.
[3] MIT Books, *Square Roots by Newton's Method*. [Online]. Available: http://www.mitpress.mit.edu/sicp/chapter1/node9.html
[4] *Underwater Acoustics Technical Guides—Speed of Sound in Seawater*. [Online]. Available: http://www.npl.co.uk/accoustics/techguides/soundseawater/speedsw.pdf
[5] M. G. Di Benedetto and G. Giancola, *Understanding Ultra Wide Band Radio Fundamentals*, ser. Prentice-Hall Communications Engineering and Emerging Technology. Englewood Cliffs, NJ: Prentice-Hall, 2004.
[6] T. S. Rappaport, *Wireless Communications: Principles and Practice*, 2nd ed. Englewood Cliffs, NJ: Prentice-Hall, 2002.
[7] I. F. Akyildiz, D. Pompili, and T. Melodia, "Underwater acoustic sensor networks: Research challenges," *J. Ad Hoc Netw.*, vol. 3, no. 3, pp. 257–279, Mar. 2005.
[8] T. C. Austin, R. P. Stokey, and K. M. Sharp, "PARADIGM: A buoy-based system for auv navigation and tracking," in *Proc. MTS/IEEE Oceans*, 2000, pp. 935–938.
[9] C. Bechaz and H. Thomas, "GIB system: The underwater GPS solution," in *Proc. 5th Eur. Conf. Underwater Acoust.*, May 2000.
[10] N. Bulusu, J. Heidemann, and D. Estrin, "GPS-less low cost outdoor localization for very small devices," *IEEE Pers. Commun.—Special Issue on Networking the Physical World*, vol. 7, no. 5, pp. 28–34, Oct. 2000.
[11] J. J. Caffery, Jr. and G. L. Stüber, "Overview of radiolocation in CDMA cellular systems," *IEEE Commun. Mag.*, vol. 36, no. 4, pp. 38–45, Apr. 1998.
[12] J. J. Caffery, Jr. and G. L. Stüber, "Subscriber location in CDMA cellular networks," *IEEE Trans. Veh. Technol.*, vol. 47, no. 2, pp. 406–416, May 1998.
[13] J. A. Catipovic, A. B. Baggeroer, K. Von Der Heydt, and D. Koelsch, "Design and performance analysis of a digital telemetry system for short range underwater channel," *IEEE J. Ocean. Eng.*, vol. OE-9, no. 4, pp. 242–252, Oct. 1984.
[14] V. Chandrasekhar and W. K. G. Seah, "An area localization scheme for underwater sensor networks," in *Proc. IEEE OCEANS Asia Pacific Conf.*, May 16–19, 2006, pp. 1–8.
[15] V. Chandrasekhar, W. K. G. Seah, Y. S. Choo, and H. V. Ee, "Localization in underwater sensor networks—Survey and challenges," in *Proc. ACM WUWNet*, 2006, pp. 33–40.
[16] X. Cheng, A. Thaeler, G. Xue, and D. Chen, "TPS: A time-based positioning scheme for outdoor wireless sensor networks," in *Proc. IEEE INFOCOM*, 2004, vol. 4, pp. 2685–2696.
[17] X. Geng and A. Zielinski, "An eigenpath underwater acoustic communication channel model," in *Proc. OCEANS, MTS/IEEE, 'Challenges Our Changing Global Environment' Conf.*, Oct. 1995, vol. 2, pp. 1189–1196.
[18] M. Hahn and J. Rice, "Undersea navigation via a distributed acoustic communication network," in *Proc. Turkish Int. Conf. Acoust.*, Jul. 4–8, 2005.
[19] W. Jobst and X. Zabalgogeazcoa, "Coherence estimates for signals propagating through acoustic channels with multiple paths," *J. Acoust. Soc. Amer.*, vol. 65, no. 3, pp. 622–630, Mar. 1979.

[20] F. Koushanfar, S. Slijepcevic, M. Potkonjak, and A. Sangiovanni-Vincentelli, "Location discovery in ad-hoc wireless sensor networks," in *Ad Hoc Wireless Networking*, X. Cheng, X. Huang, and D.-Z. Du, Eds. Norwell, MA: Kluwer, 2003, pp. 137–173.
[21] Q. Liang, S.W. Samn, and X. Cheng, "Outdoor UWB channel modeling in rich scattering and time-varying environment," *IEEE Trans. Wireless Commun.,* submitted for publication.
[22] F. Liu, X. Cheng, D. Hua, and D. Chen, "Range-difference based location discovery for sensor networks with short range beacons," *Int. J. Ad Hoc Ubiquitous Comput.,* to be published.
[23] G. Loubet and B. Faure, "Characterization of the underwater channel for acoustic communications," *J. Acoust. Soc. Amer.*, vol. 105, no. 2, p. 1364, Feb. 1999.
[24] A. Nasipuri and K. Li, "A directionality based location discovery scheme for wireless sensor networks," in *Proc. WSNA*, 2002, pp. 105–111.
[25] D. Niculescu and B. Nath, "Ad hoc positioning system (APS)," in *Proc. IEEE GLOBECOM*, 2001, pp. 2926–2931.
[26] J. Partan, J. Kurose, and B. N. Levine, "A survey of practical issues in underwater networks," in *Proc. 1st ACM Int. Workshop Underwater Netw., Int. Conf. Mobile Comput. Netw.*, Los Angeles, CA, Sep. 2006, pp. 17–24.
[27] A. A. Saleh and R. A. Valenzuela, "A statistical model for indoor multipath propagation," *IEEE J. Sel. Areas Commun.*, vol. JSAC-5, no. 2, pp. 128–137, Feb. 1987.
[28] G. H. Sandsmark and A. Solstad, "Adaptive beam forming and adaptive equalization for high-speed underwater acoustic data transmission," in *Proc. Underwater Defence Tech. Conf.*, Apr. 1991, pp. 707–712.
[29] A. Syed and J. Heidemann, "Time synchronization for high latency acoustic networks," in *Proc. IEEE INFOCOM*, 2006, pp. 1–12.
[30] A. Thaeler, M. Ding, and X. Cheng, "iTPS: An improved location discovery scheme for sensor networks with long range beacons," *J. Parallel Distrib. Comput.*, vol. 65, no. 2, pp. 98–106, Feb. 2005.
[31] Y. Zhang and L. Cheng, "A distributed protocol for multi-hop underwater robot positioning," in *Proc. IEEE Int. Conf. Robot. Biometr.*, Aug. 2004, pp. 480–484.
[32] Z. Zhou, J.-H. Cui, and S. Zhou, "Localization for large-scale underwater sensor networks," Univ. Connecticut, CSE Tech. Rep.: UbiNet-TR06-04, Dec. 2006.

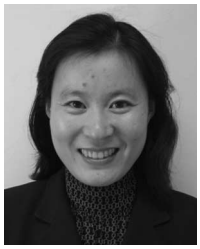

Xiuzhen (Susan) Cheng (M'03) received the M.S. and Ph.D. degrees in computer science from the University of Minnesota, Minneapolis, in 2000 and 2002, respectively.

In 2006, she was a Program Director with the National Science Foundation (NSF) for six months. She is currently an Assistant Professor with the Department of Computer Science, The George Washington University, Washington, DC. Her current research interests include wireless and mobile computing, sensor networking, wireless and mobile security, and approximation algorithm design and analysis.

Dr. Cheng has served on the editorial boards of several technical journals and in the technical program committees of various professional conferences/workshops. She was the Program Cochair of the first International Conference on Wireless Algorithms, Systems, and Applications (WASA06). She was the recipient of the NSF CAREER Award in 2004.

Haining Shu (S'04) received the B.S. degree in electronics and information systems from Peking University, Beijing, China, in 1996, the M.S. degree in electrical engineering from the University of Texas at Dallas, Richardson, in 2002, and the Ph.D. degree in electrical engineering from The University of Texas, Arlington, in 2007.

Prior to the master program, she was a System Engineer with the Telecom Planning and Research Institute, Beijing. She is currently with the Department of Electrical Engineering, The University of Texas at Arlington. Her research interests include fuzzy logic systems and applications, distributed source coding, sensor networks, and collaborative radar systems.

Qilian Liang (M'01–SM'05) received the B.S. degree from Wuhan University, Wuhan, China, in 1993, the M.S. degree from Beijing University of Posts and Telecommunications, Beijing, China, in 1996, and the Ph.D. degree from the University of Southern California (USC), Los Angeles, in 2000, all in electrical engineering.

In August 2002, he joined the Department of Electrical Engineering, The University of Texas at Arlington (UTA). He was a member of Technical Staff with Hughes Network Systems Inc., San Diego, CA. He has published more than 120 journal and conference papers and six book chapters. He is the holder of six pending U.S. patents. His research interests include sensor networks, wireless communications, wireless networks, communication systems and communication theory, signal processing for communications, fuzzy logic systems and applications, and collaborative and distributed signal processing.

Dr. Liang was the recipient of the 2002 IEEE TRANSACTIONS ON FUZZY SYSTEMS Outstanding Paper Award, the 2003 U.S. Office of Naval Research Young Investigator Award, and the 2005 UTA College of Engineering Outstanding Young Faculty Award.

David Hung-Chang Du (S'81–M'81–SM'95–F'98) received the B.S. degree in mathematics from National Tsing Hua University, Hsinchu, Taiwan, R.O.C., in 1974 and the M.S. and Ph.D. degrees in computer science from the University of Washington, Seattle, in 1980 and 1981, respectively.

He is currently a Qwest Chair Professor with the Department of Computer Science and Engineering, University of Minnesota, Minneapolis. He has authored and coauthored more than 190 technical papers, including 90 referred journal publications in his research areas. He has also graduated 48 Ph.D. and 80 M.S. students. His research interests include cyber security, sensor networks, multimedia computing, storage systems, high-speed networking, high-performance computing over clusters of workstations, database design, and computer-aided design for very-large-scale integration circuits.

Dr. Du is a Fellow of the Minnesota Supercomputer Institute. He is currently serving on a number of journal editorial boards. He has also served as guest editor for a number of journals, including IEEE Computer, and *Communications of ACM*. He has also served as Conference Chair and Program Committee Chair for several conferences in the multimedia, database, and networking areas.